

**UCC Library and UCC researchers have made this item openly available.
Please [let us know](#) how this has helped you. Thanks!**

Title	Subwavelength grating-based spiral metalens for tight focusing of laser light
Author(s)	Kotlyar, Victor V.; Stafeev, Sergey S.; Nalimov, Anton G.; O'Faolain, Liam
Publication date	2019-04-12
Original citation	Kotlyar, V. V., Stafeev, S. S., Nalimov, A. G. and O'Faolain, L. (2019) 'Subwavelength grating-based spiral metalens for tight focusing of laser light', Applied Physics Letters, 114(14), 141107 (5pp). doi: 10.1063/1.5092760
Type of publication	Article (peer-reviewed)
Link to publisher's version	http://dx.doi.org/10.1063/1.5092760 Access to the full text of the published version may require a subscription.
Rights	© 2019, the Authors. Published by AIP Publishing. This article may be downloaded for personal use only. Any other use requires prior permission of the author and AIP Publishing. This article appeared as Kotlyar, V. V., Stafeev, S. S., Nalimov, A. G. and O'Faolain, L. (2019) 'Subwavelength grating-based spiral metalens for tight focusing of laser light', Applied Physics Letters, 114(14), 141107 (5pp). doi: 10.1063/1.5092760 and may be found at https://doi.org/10.1063/1.5092760
Embargo information	Access to this article is restricted until 12 months after publication by request of the publisher.
Embargo lift date	2020-04-12
Item downloaded from	http://hdl.handle.net/10468/7875

Downloaded on 2020-06-06T01:51:06Z



UCC

University College Cork, Ireland
Coláiste na hOllscoile Corcaigh

Subwavelength grating-based spiral metalens for tight focusing of laser light

Cite as: Appl. Phys. Lett. **114**, 141107 (2019); <https://doi.org/10.1063/1.5092760>

Submitted: 14 February 2019 . Accepted: 27 March 2019 . Published Online: 12 April 2019

Victor V. Kotlyar , Sergey S. Stafeev , Anton G. Nalimov , and Liam O'Faolain 



View Online



Export Citation



CrossMark

ARTICLES YOU MAY BE INTERESTED IN

[Tamm phonon-polaritons: Localized states from phonon-light interactions](#)

Applied Physics Letters **114**, 141101 (2019); <https://doi.org/10.1063/1.5089693>

[Exclusive generation of orbital angular momentum modes in parity-time symmetry fiber gratings](#)

Applied Physics Letters **114**, 141103 (2019); <https://doi.org/10.1063/1.5087116>

[Enhancement of resolution in microspherical nanoscopy by coupling of fluorescent objects to plasmonic metasurfaces](#)

Applied Physics Letters **114**, 131101 (2019); <https://doi.org/10.1063/1.5066080>

Subwavelength grating-based spiral metalens for tight focusing of laser light

Cite as: Appl. Phys. Lett. **114**, 141107 (2019); doi: [10.1063/1.5092760](https://doi.org/10.1063/1.5092760)

Submitted: 14 February 2019 · Accepted: 27 March 2019 ·

Published Online: 12 April 2019



View Online



Export Citation



CrossMark

Victor V. Kotlyar,^{1,2}  Sergey S. Stafeev,^{1,2,a)}  Anton G. Nalimov,^{1,2}  and Liam O'Faolain^{3,4} 

AFFILIATIONS

¹Image Processing Systems Institute of the RAS-Branch of Federal Scientific Research Center Crystallography and Photonics of the Russian Academy of Science, 151 Molodogvardeyskaya St., Samara 443001, Russia

²Samara National Research University, 34 Moskovskoe Shosse, Samara 443086, Russia

³Centre for Advanced Photonics and Process Analysis, Cork Institute of Technology, Cork T12 P928, Ireland

⁴Tyndall National Institute, Cork T12R5CP, Ireland

^{a)}sergey.stafeev@gmail.com

ABSTRACT

In this paper, we investigate a 16-sector spiral metalens fabricated on a thin film (130 nm) of amorphous silicon, consisting of a set of subwavelength binary diffractive gratings and with a numerical aperture that is close to unity. The metalens converts linearly polarized incident light into an azimuthally polarized optical vortex and focuses it at a distance approximately equal to the wavelength of the incident light, $\lambda = 633$ nm. Using a scanning near-field optical microscope, it is shown experimentally that the metalens forms an elliptical focal spot with diameters smaller than the diffraction limit: $\text{FWHM}_x = 0.32\lambda$ ($\pm 0.03\lambda$) and $\text{FWHM}_y = 0.51\lambda$ ($\pm 0.03\lambda$). The experimental results are close to those of a numerical simulation using the FDTD method, with $\text{FWHM}_x = 0.37\lambda$ and $\text{FWHM}_y = 0.49\lambda$. The technological errors due to manufacturing were taken into account in the simulation. This is the smallest focal spot yet obtained with a metalens.

Published under license by AIP Publishing. <https://doi.org/10.1063/1.5092760>

A significant number of recent scientific papers have been devoted to the investigation of metasurfaces, thin optical elements that simultaneously control the amplitude, phase, and polarization of propagated light.^{1,2} Metasurface-based elements can focus light into a ring,³ a segment,⁴ or a spot.^{5–10} A special case of a metasurface is a simple subwavelength grating.

In previous work, we have investigated metalenses based on subwavelength gratings.¹¹ These subwavelength gratings are anisotropic, meaning that TE- and TM-polarized waves that propagated through them have different phases. Based on this effect, it is possible to create analogs of the classical half-wave plates, which rotate the direction of polarization. The spatial orientation of these wave plates will be determined by the direction of the relief of the grating. Since the relief of a diffractive element may be oriented in any direction, it is possible to create subwavelength grating-based elements that convert a linearly polarized beam into a beam with a spatially inhomogeneous direction of polarization (i.e., one that varies at different points in the cross section of the beam). In prior work, we have also investigated elements based on subwavelength gratings that are designed to produce cylindrical vector beams (CVBs), that is, beams in which the direction of polarization has radial symmetry.¹²

Although CVBs have been known in optics for a long time, numerous studies of these are ongoing. For example, in Ref. 13, a compact element on a chip was proposed for the generation of CVB. The scattering of radially and azimuthally polarized light on Mie particles was investigated in Ref. 14. Radially or azimuthally polarized light is very often used in the tight focusing of laser light; for example, a method for obtaining optical needles using radially polarized light was proposed in Ref. 15, in which the obtained spot had a depth of $\text{DOF} = 53\lambda$ (where DOF is the Depth of Focus) and a subwavelength diameter of $\text{FWHM} = 0.8\lambda$ (FWHM is the Full Width at Half Maximum). An optical needle with a smaller diameter was obtained in Ref. 16, in which the $\text{FWHM} = 0.414\lambda$ and the $\text{DOF} = 7.58\lambda$. Other papers on obtaining a subwavelength focus are presented in Refs. 17–19. In previous work,²⁰ we proposed a four-sector subwavelength grating that rotates the direction of polarization of linearly polarized light through angles of 45° , -45° , 135° , and -135° . The metalens investigated in Ref. 21 combined the Fresnel zone plate and the four-sector radial polarizer from Ref. 20. The main drawback of the system in Refs. 20 and 21 is that the direction of polarization of the light propagated through the element does not change continuously and is limited to four directions by the number of zones. The investigation in Ref. 22 was devoted to a numerical investigation of the influence of the

number of sectors on the results of focusing. The present work continues the authors' investigations in Refs. 22 and 23.

In this work, we investigate a 16-sector spiral metalens consisting of subwavelength gratings. This metalens converts linearly polarized light into an azimuthally polarized optical vortex and focuses it. Using a scanning near-field optical microscope (SNOM), it is shown experimentally that the metalens forms a focal spot with diameters smaller than the diffraction limit: $\text{FWHM}_x = 0.32\lambda$ and $\text{FWHM}_y = 0.51\lambda$. The half-maximum area (HMA) of the focal spot is equal to $\text{HMA} = 0.128\lambda^2$. This is the smallest focal spot obtained using a metalens (the smallest focal spot obtained previously was reported in Ref. 6, with $\text{FWHM} = 0.57\lambda$). The experimentally obtained values are close to the results of a numerical simulation (using the FDTD method) of the manufactured metalens, with $\text{FWHM}_x = 0.37\lambda$ and $\text{FWHM}_y = 0.49\lambda$. The half-maximum area of the spot is $\text{HMA} = 0.142\lambda^2$. Moreover, if the metalens could be made without technological errors, the diameters of the focal spot would be 0.435λ and 0.457λ , and its area would be $\text{HMA} = 0.156\lambda^2$. In this case, the focal spot of the ideally manufactured metalens would be almost round but would have a larger area. It should be noted that the theoretical limit on the focal spot area of the zone plate is $\text{HMA} = 0.154\lambda^2$ (Ref. 24) (our metalens produces a focal spot with $\text{HMA} = 0.156\lambda^2$). Previously, the smallest focal spot area was produced using a parabolic mirror in Ref. 25 and was equal to $\text{HMA} = 0.134\lambda^2$; our metalens produces a smaller focal spot ($\text{HMA} = 0.128\lambda^2$). A similar focal spot area is formed by a diffraction axicon with a period equal to the illuminating wavelength.²⁶ Note that in this work, we do not draw a comparison with the metalenses designed by use of a superoscillation phenomenon,^{17,27} because the said method has an unprecedentedly low efficiency. It has been reported that the intensity of a focal spot 160 nm (0.27λ) in diameter is just 10^{-5} of the background intensity.¹⁷ Meanwhile, the metalens proposed in this paper is able to generate a focal spot whose intensity is seven times that of the incident beam.

This spiral metalens [Fig. 1(a)] is a combination of a spiral zone plate with a topological charge $m = 1$ [Fig. 1(b)] and a sectorial subwavelength grating that acts as a half-wave plate. The lens consists of 16 radial sectors, each of which rotates the polarization of the incident light to produce the azimuthal polarization [Fig. 1(c)]. Each sector is divided into sub-areas in the shape of a circular arc. The angle of the relief in neighboring areas within one sector is chosen such that the

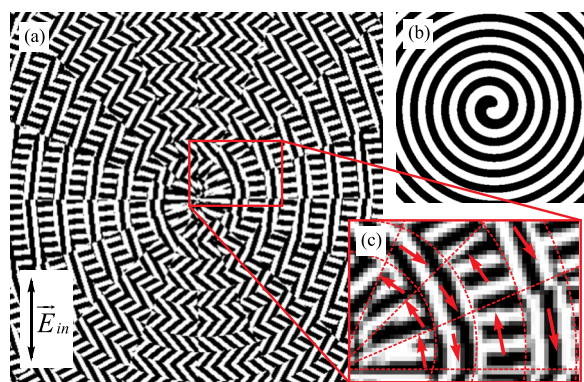


FIG. 1. (a) Spiral metalens (the image size is $8\ \mu\text{m} \times 8\ \mu\text{m}$) and (b) corresponding binary spiral zone plates with topological charge $m = 1$; (c) polarization of light transmitted through the metalens.

polarization of the light passing through them differs by π [Fig. 1(c)]. Linearly polarized incident light (the incident polarization in Fig. 1 is directed vertically) is transformed into a focused, azimuthally polarized optical vortex. The period of the grating is 220 nm, and the depth of the relief is 120 nm. The focal length of the zone plate [shown in Fig. 1(b)] is equal to the illumination wavelength, $f = \lambda = 633\ \text{nm}$. Figure 1(c) also shows that the direction of the grating relief in the adjacent areas of the lens is mutually perpendicular.

A series of simulations were carried out using the FDTD method implemented in FullWave software. The parameters for these simulations are as follows: the wavelength was $\lambda = 633\ \text{nm}$, the size of the entire simulated area was $8 \times 8 \times 2\ \mu\text{m}^3$, and the simulation mesh step was $\lambda/30$ along all three axes. The index of refraction of the metalens was $n = 4.352 + 0.486i$ (amorphous silicon). Figure 2 shows the intensity distribution at the focal spot calculated using the FDTD method.

The metalens forms an almost circular focal spot at a distance of 600 nm from the surface. The diameters of the focal spot (Fig. 2) formed by the ideal metalens [Fig. 1(a)] are $\text{FWHM}_x = 0.435\lambda$ and $\text{FWHM}_y = 0.457\lambda$.

Figure 2(c) depicts the phase pattern of a light field behind the metalens in Fig. 1. Two spirals shown as dashed white and black lines are present in Fig. 2(c), with each turn of the spirals characterized by two phase jumps by π . Such a behavior of the phase is the result of superposition of an optical vortex with topological charge 1 and the amplitude $\exp(i\varphi)$ and a plane azimuthally polarized wave described

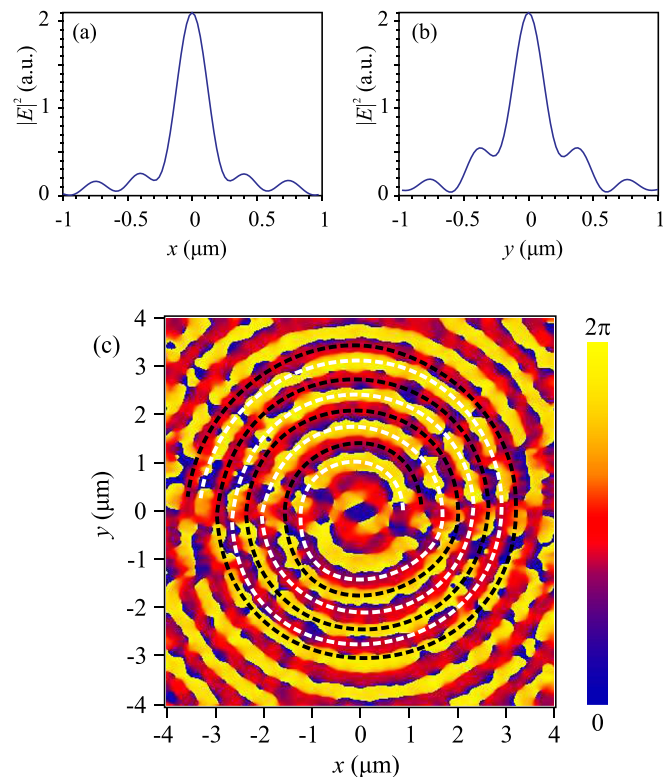


FIG. 2. Calculated intensity in the focal spot when an ideal metalens (Fig. 1) is illuminated by linearly polarized laser light: along the (a) x -axis, (b) y -axis, and (c) the phase pattern of the component E_x calculated $0.1\ \mu\text{m}$ behind the metalens.

by the Jones vector $\begin{pmatrix} -\sin \varphi \\ \cos \varphi \end{pmatrix}$. In the superposition, the transverse electric field components E_x and E_y (the longitudinal component is absent) are described by an amplitude $A(r) \exp(2i\varphi) + B(r)$, where the functions $A(r)$ and $B(r)$ depend only on the radial coordinate. Although both projections of the electric field have a vortex component $\exp(2i\varphi)$ [Fig. 2(c)], the intensity $I = |E_x|^2 + |E_y|^2$ is independent of the azimuthal angle φ and circularly symmetrical, taking its maximum value at the center [Figs. 2(a) and 2(b)].

A metalens with the relief shown in Fig. 1(a) was fabricated using electron beam lithography. A 130 nm-thick amorphous silicon film (a-Si) (with refractive index $n = 4.35 + i0.486$) was deposited on a transparent Pyrex substrate (with refractive index $n = 1.5$), coated with a 320 nm-thick polymethyl methacrylate (PMMA) resist, and baked at a temperature of 180 °C. The thickness of the resist was chosen to give a combination of good etch resistance and high-resolution patterning. To prevent charging, the surface was sputtered with a gold layer of 15 nm thickness. A binary template was transferred onto the resist surface using a 30 kV electron beam. The specimen was developed in water blended with isopropanol in the ratio 3:7, and the template was then transferred from the resist into the a-Si film, using reactive ion etching in a gaseous atmosphere of CHF_3 and SF_6 . The aspect ratio of the etch rate of the material and the photomask was found to be 1:2.5.

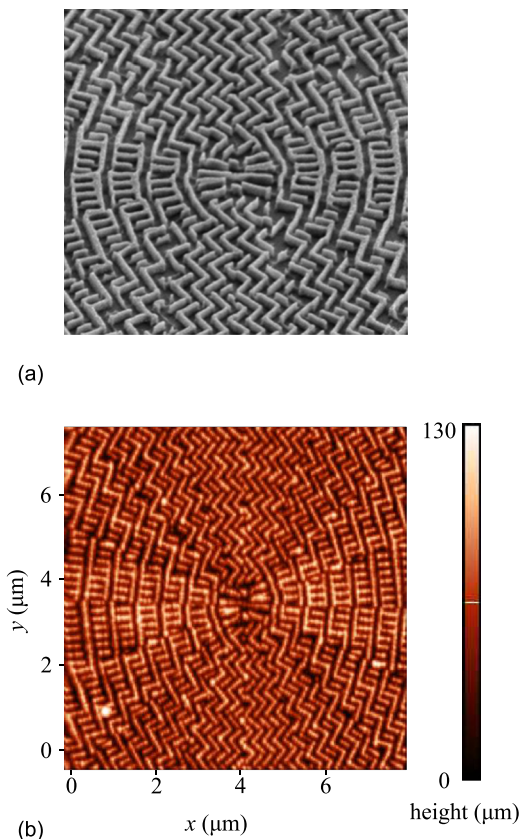


FIG. 3. (a) Electron microscopy (the image size is $4 \mu\text{m} \times 4 \mu\text{m}$) and (b) atomic force microscopy images of a spiral metalens in an a-Si film.

The height of the metalens microrelief is 130 nm, being equal to the thickness of the amorphous silicon film. Electron microscopy and atomic force microscopy images are shown in Fig. 3. As a result of this process, the gold was completely washed out from the PMMA surface.

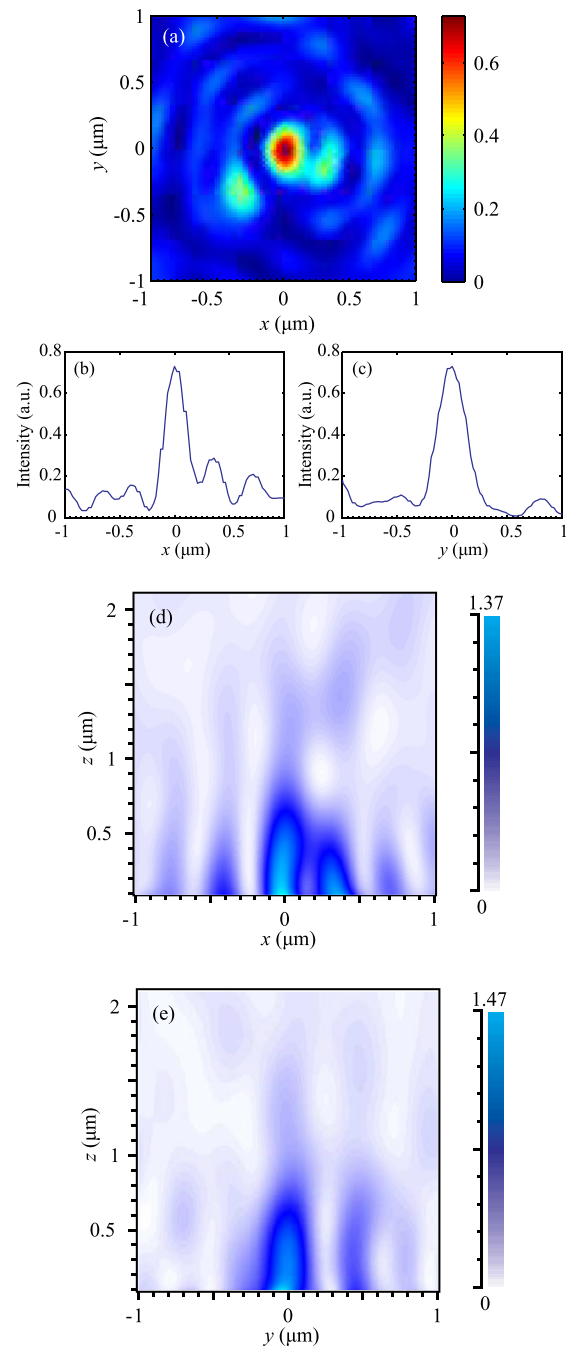


FIG. 4. Calculated intensity of the focal spot: 2D intensity pattern (a) and intensity profiles along the (b) x - and (c) y -axes. Numerically simulated near-focus intensity patterns in two longitudinal planes: (d) XZ-plane and (e) YZ-plane.

Next, we conducted a FDTD-aided simulation of the propagation of light through the metalens with the manufactured relief shown in Fig. 3. The focal length in this simulation was equal to 633 nm. Figure 4 shows the intensity distribution of the focal spot.

From Figs. 4(a) and 4(b), the transverse size of the focal spot is seen to be $\text{FWHM}_x = 0.37\lambda$ and $\text{FWHM}_y = 0.49\lambda$, with Figs. 4(d) and 4(e) showing that the depth of focus at full width of half-maximum intensity is approximately $\text{DOF} = 700$ nm.

The focusing by the fabricated spiral metalens was investigated experimentally using a scanning near-field optical microscope (Ntegra Spectra, NT-MDT). Figure 5 shows the experimental setup. In this experiment, a light beam from an He-Ne laser (wavelength 633 nm) was used to illuminate the metalens. The full width of the incident beam was $30\ \mu\text{m}$. The intensity of the focal spot was measured using a hollow, pyramid-shaped probe (C) with a 100 nm pinhole in the vertex. After passing through the pinhole, the light was collected by a $100\times$ objective lens (O_1) before traveling through the spectrometer (S) (Solar TII, Nanofinder 30) to the CCD camera (Andor, DV401-BV).

Figure 6 shows the results of focusing. The intensity distribution is shown in Fig. 6(a), and its sections along the x and y axes are shown in Figs. 6(b) and 6(c), respectively. The focal spot diameters in Fig. 6 were $\text{FWHM}_x = 0.32\lambda$ [Fig. 6(b)] and $\text{FWHM}_y = 0.51\lambda$ [Fig. 6(c)]. The maximum intensity of the focal spot was seven times larger than the maximum intensity of the input beam.

In this work, we investigate a 16-sector spiral metalens consisting of subwavelength gratings. The metalens converts linearly polarized light into an azimuthally polarized optical vortex with topological charge $m = 1$ and focuses it. The metalens was fabricated using electron beam lithography applied to an amorphous silicon film deposited on a Pyrex substrate. Using a scanning near-field optical microscope, it was shown experimentally that the metalens forms a focal spot with diameters that are smaller than the diffraction limit: $\text{FWHM}_x = 0.32\lambda$ and $\text{FWHM}_y = 0.51\lambda$. The experimentally obtained values are close to the results of a numerical simulation of the manufactured metalens using the FDTD method, which are $\text{FWHM}_x = 0.37\lambda$ and $\text{FWHM}_y = 0.49\lambda$. Moreover, if the metalens could be made without technological errors, the focal spot diameters would be equal to 0.435λ and 0.457λ . It should be noted that the experimental size of the focal spot along the horizontal axis (0.32λ) is less than the diffraction limit of the focus formed by an annular aperture (0.36λ). This diffraction limit coincides with the

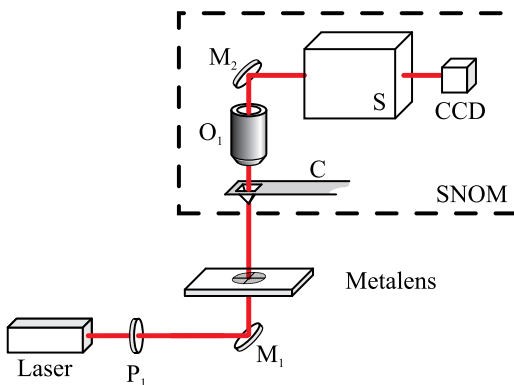


FIG. 5. Experimental setup: P_1 —linear polarizer; M_1 , M_2 —mirrors; O_1 — $100\times$ objective lens; C—probe; S—spectrometer; and CCD—CCD camera.

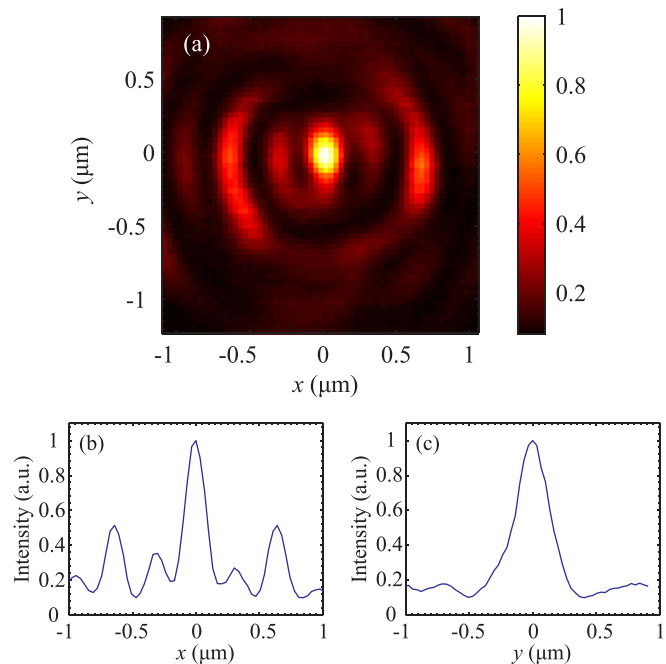


FIG. 6. Measured intensity of the focal spot of the metalens (Fig. 3): 2D intensity pattern (a) and intensity profiles along the (b) x - and (c) y -axes.

diameter of a Bessel beam of zero order. The side lobes of the Bessel beam are equal to 16% of the maximum intensity. As can be seen from Fig. 6, the side lobes of the focal spot have an intensity that is almost 50% of the maximum.

This work was funded by the Russian Science Foundation (Project No. 18-19-00595) in the part of experiment and by the Ministry of Science and Higher Education of Russian Federation (Agreement No. 007-Г3/У3363/26) in the part of numerical simulation.

REFERENCES

- ¹N. Yu and F. Capasso, *Nat. Mater.* **13**(2), 139 (2014).
- ²Q. He, S. Sun, S. Xiao, and L. Zhou, *Adv. Opt. Mater.* **6**, 1800415 (2018).
- ³L. Lan, W. Jiang, and Y. Ma, *Appl. Phys. Lett.* **102**(23), 231119 (2013).
- ⁴L. Verslegers, P. B. Catrysse, Z. Yu, J. S. White, E. S. Barnard, M. L. Brongersma, and S. Fan, *Nano Lett.* **9**(1), 235 (2009).
- ⁵F. Aieta, P. Genevet, M. A. Kats, N. Yu, R. Blanchard, Z. Gaburro, and F. Capasso, *Nano Lett.* **12**(9), 4932 (2012).
- ⁶A. Arbabi, Y. Horie, A. J. Ball, M. Bagheri, and A. Faraon, *Nat. Commun.* **6**, 7069 (2015).
- ⁷A. Arbabi, Y. Horie, M. Bagheri, and A. Faraon, *Nat. Nanotechnol.* **10**(11), 937 (2015).
- ⁸X. Ni, S. Ishii, A. V. Kildishev, and V. M. Shalaev, *Light Sci. Appl.* **2**(4), e72 (2013).
- ⁹P. R. West, J. L. Stewart, A. V. Kildishev, V. M. Shalaev, V. V. Shkunov, F. Strohkendl, Y. A. Zakharenkov, R. K. Dodds, and R. Byren, *Opt. Express* **22**(21), 26212 (2014).
- ¹⁰D. Lin, P. Fan, E. Hasman, and M. L. Brongersma, *Science* **345**(6194), 298 (2014).
- ¹¹S. S. Stafeev, V. V. Kotlyar, A. G. Nalimov, M. V. Kotlyar, and L. O'Faolain, *Photonics Nanostruct. Fundam. Appl.* **27**, 32 (2017).
- ¹²Q. Zhan, *Adv. Opt. Photonics* **1**, 1 (2009).
- ¹³Z. Shao, J. Zhu, Y. Zhang, Y. Chen, and S. Yu, *Opt. Lett.* **43**, 1263 (2018).
- ¹⁴A. K. Singh, S. Saha, S. D. Gupta, and N. Ghosh, *Phys. Rev. A* **97**, 043823 (2018).
- ¹⁵R. Martínez-Herrero, D. Maluenda, I. Juvells, and A. Carnicer, *Sci. Rep.* **8**, 2657 (2018).

- ¹⁶C. Shi, Z. Nie, Y. Tian, C. Liu, Y. Zhao, and B. Jia, *Optoelectron. Lett.* **14**(1), 1 (2018).
- ¹⁷K. S. Rogers, K. N. Bourdakos, G. H. Yuan, S. Mahajan, and E. T. F. Rogers, *Opt. Express* **26**(7), 8095 (2018).
- ¹⁸J. Guan, J. Lin, C. Chen, Y. Ma, J. Tan, and P. Jin, *Opt. Commun.* **404**, 118 (2017).
- ¹⁹H.-F. Xu, Y. Zhou, H.-W. Wu, H.-J. Chen, Z.-Q. Sheng, and J. Qu, *Opt. Express* **26**(16), 20076 (2018).
- ²⁰S. S. Stafeev, L. O'Faolain, V. V. Kotlyar, and A. G. Nalimov, *Appl. Opt.* **54**, 4388 (2015).
- ²¹V. V. Kotlyar, A. G. Nalimov, S. S. Stafeev, C. Hu, L. O'Faolain, M. V. Kotlyar, D. Gibson, and S. Song, *Opt. Express* **25**, 8158 (2017).
- ²²A. G. Nalimov and V. V. Kotlyar, *Optik* **159**, 9 (2018).
- ²³V. V. Kotlyar and A. G. Nalimov, *Comput. Opt.* **41**(5), 645 (2017).
- ²⁴N. Davidson and N. Bokor, *Opt. Lett.* **29**(12), 1318 (2004).
- ²⁵J. Stadler, C. Stanciu, C. Stupperich, and A. J. Meixner, *Opt. Lett.* **33**(7), 681 (2008).
- ²⁶V. V. Kotlyar, S. S. Stafeev, A. A. Kovalev, and A. G. Nalimov, *Comput. Opt.* **36**(2), 183 (2012).
- ²⁷T. Roy, E. T. F. Regers, and N. I. Zheludev, *Opt. Express* **21**(6), 7577 (2013).